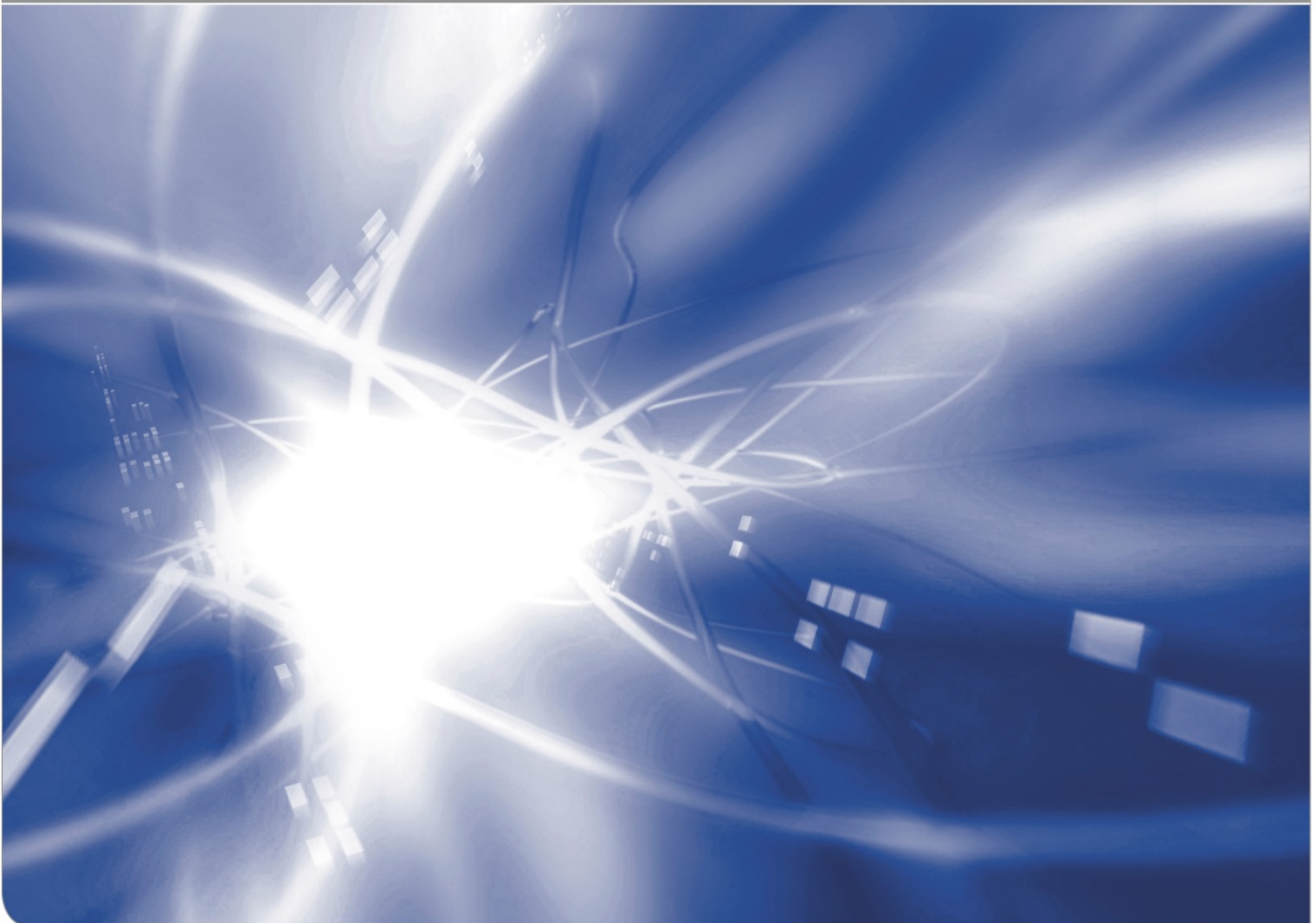


# Hydroxyl concentrations on crack surfaces from measurements by Tomozawa, Han and Lanford

G. Schell, G. Rizzi, T. Fett

KIT SCIENTIFIC WORKING PAPERS 82



Institut für Angewandte Materialien, Karlsruher Institut für Technologie (KIT)

### Impressum

Karlsruher Institut für Technologie (KIT)  
www.kit.edu



This document is licensed under the Creative Commons Attribution – Share Alike 4.0 International License (CC BY-SA 4.0): <https://creativecommons.org/licenses/by-sa/4.0/deed.en>

2018

ISSN: 2194-1629

## **Abstract**

The effect of stress-enhanced hydroxyl concentration in silica penetrated by water could be proved by using hydrogen measurements from literature (Tomozawa, Han and Lanford 1991). The concentration of water penetrated into silica during a subcritical crack growth test is strongly larger than the water diffused into unstressed silica surfaces. From this result it could be concluded that the equilibrium constant of the water-silica reaction is strongly enhanced due to the near-tip tensile stresses of cracks and that the reaction volume change is **positive**.



# Contents

<b>1 Theoretical considerations</b>	1
<b>2 Water concentration at crack surfaces of subcritically grown cracks</b>	1
2.1 Experimental data	1
2.2 Computation of the equilibrium constant	3
<b>3 Sign of the reaction volume</b>	5
<b>4 Etching</b>	6
<b>APPENDIX</b>	8
<b>References</b>	10



## 1 Introduction

The classic work on the effect of pressure on the equilibrium constant of a chemical reaction was done by Le Chatelier [1]. From his work, it is well known that chemical reactions that exhibit a change in volume will be sensitive to the ambient pressure of the reaction. Changing the pressure changes the equilibrium constant of the reaction and hence the ratio of the concentration of reaction products to reactants. According to Doremus [2], water penetrates into silica glass by the diffusion of molecular water.

At temperatures  $T < 450^\circ\text{C}$ , the equilibrium constant  $k$  of reaction



is

$$k = \frac{S}{C}. \quad (2)$$

Whereas the molecular water,  $C$ , can move by diffusion, the hydroxyls,  $S$ , are immobile. Only those hydroxyls can react in the reverse reaction step, which are directly neighboring. Consequently, the reaction is of first order. The question in which way the equilibrium constant depends on stresses is discussed in literature controversially. Whereas in [3] an increase of  $k$  was found under tension, it is claimed in [4] that  $k$  would decrease. In the present analysis of data measured on crack surfaces after sub-critical crack growth by Tomozawa et al. [5], it will be shown that  $k$  must increase under tensile stresses.

## 2 Water concentration at crack surfaces of subcritically grown cracks

### 2.1 Experimental data

An interesting experiment was performed by Tomozawa et al. [5]. Fracture surfaces were formed by the passage of a crack through Double Cleavage Drilled Compression specimens (DCDC) [6, 7], while the specimen was exposed to water. The experiments demonstrated that the surface concentration of water was significantly higher near the fracture surface than would be the case for silica glass merely exposed to water for a time equal to that required for the passage of the crack through the specimen.

The study [5] used nuclear reaction analysis (NRA) to determine the concentration profile of water near the fracture surface of the glass. This technique provides a direct chemical analysis of the concentration of H as a function of distance from the fracture surface. A “finite depth resolution of the technique is caused by a Doppler energy shift resulting from thermal vibration of hydrogen bound in the sample, by the finite energy spread of the  $^{15}\text{N}$  beam, by fluctuations in the energy loss of the  $^{15}\text{N}$  ions in the target, and by several smaller effects” [5].

In Fig. 1 the results from [5] are plotted versus depth (circles). We included also the high values from Fig. 3 in [5] (indicated by squares in Fig. 1).

It should be noted that the measured data are affected by the finite breadth of the instrument curve. A detailed analysis that includes the effect of the rather large breadth of the instrumental is given by Wiederhorn et al. [8]. Here, we are interested only in the surface values for which the effect of the instrument curve is of minor importance.

This technique indicated hydrogen concentrations of the order of  $10^{22}$  atoms/cm<sup>3</sup> at the surface of the glass. In contrast to this result, Zouine et al. [9] found for the H-concentration at room temperature ( $23^\circ\text{C}$ ,  $p=2.8$  kPa water vapour pressure, absence of applied stresses)

$$c_H = 1.4 \times 10^{20} \text{ atoms/cm}^3 \quad (3)$$

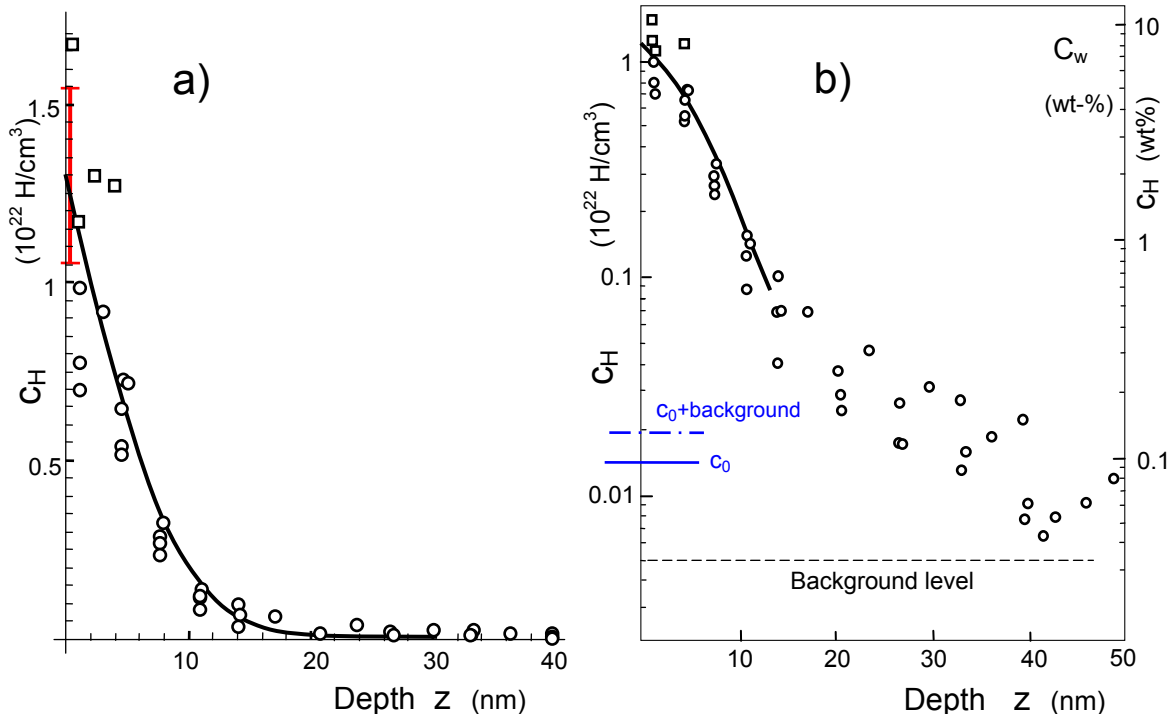


**Fig. 1** Hydrogen concentration in the surface region of a growing crack via NRA-measurements by Tomozawa et al.[5] (circles: from Fig. 4, squares: from Fig. 3 in [5]); a) linear ordinate: curve given by eq.(4), red bar indicates 90%-Confidence Interval of the surface concentration, b) logarithmic ordinate.

In order to allow an approximate extrapolation of measured data to the surface, we fitted the data  $c_H$  in Fig. 1 arbitrarily by a complementary error function

$$c_H = c_{H,0} \operatorname{erfc}\left[\frac{z}{2b}\right] + \underbrace{0.005 \times 10^{22} / \text{cm}^3}_{\text{Background}} \quad (4)$$

taking into account the background level of  $0.005 \cdot 10^{22}/\text{cm}^3$ . The coefficient  $c_{\text{H},0}$  is the concentration for a stress-free surface.

By fitting (4) to the measurements, the best set of parameters was found as

$$c_{\text{H},0}=1.30 [1.055, 1.55] \cdot 10^{22}/\text{cm}^3, b=4.95 [3.28, 6.61] \text{ nm}^{-1} \text{ (90\% CI).}$$

with the 90%-Confidence Intervals in brackets. The red bar in Fig. 1a indicates the 90%-CI of the surface concentration. The depth  $b$  at which the concentration decreased to  $\cong 50\%$  of the surface value in Fig. 1a is about 5 nm.

As there are two hydrogen atoms for each water molecule, the surface concentration of water is one-half this value. The right ordinate in Fig. 1b represents the total water concentration.

Using Avogadro's number,  $N=6.02 \times 10^{23}$  molecules/mol gives for the water concentration in molar units:

$$C_w = \frac{c_{\text{H}}}{2N} \quad (5)$$

The surface value is

$$C_w(0) = \frac{c_{\text{H}}}{2N} = 0.0108 [0.0095, 0.0121] \text{ (mole/cm}^3\text{)} \quad (6)$$

With  $\rho=2.2 \text{ g/cm}^3$  for the density of silica glass [10] and a molecular mass of water of  $m_{\text{H}_2\text{O}}=18 \text{ g/mol}$ , the water concentration at the surface of the glass is in mass units

$$C_w(0) = \frac{c_{\text{H}}}{2N} \frac{m_{\text{H}_2\text{O}}}{\rho} = 8.8 [7.7, 9.8] \text{ (wt\%)} \quad (7)$$

From the result by Zouine et al. [9] for unstressed silica surfaces in water,  $c_{\text{H},0}=1.4 \cdot 10^{20}$  H-atoms, the water concentration in the absence of stress,  $C_{w,0}$ , reads

$$C_{w,0} = 0.000116 \text{ (mole/cm}^3\text{)} = 0.095 \text{ (wt \%)} \quad (8)$$

The value of  $c_0$  is shown by the blue line in Fig. 1 and after including the background by the dash dotted line. From these results, an increase of the water concentration by a factor of  $C_w(0)/C_{w,0}=93$  has to be concluded.

## 2.2 Computation of the equilibrium constant

In molar units, the total water concentration is given by

$$C_w = C + \frac{1}{2}S = C(1 + \frac{1}{2}k) \quad (9)$$

where the quantity  $k$  is the equilibrium constant given by eq.(2). For the case of saturation, the surface concentration of molecular water,  $C(0)$  is generally *assumed* to de-

pend only on the water vapour pressure in the environment,  $C(0)=C_0=\text{const}$ . This leads to

$$C_w = C_0 + \frac{1}{2}S = C_0(1 + \frac{1}{2}k) \quad (10)$$

In the absence of stresses, the equilibrium constant may be denoted as  $k_0$ . In this case, the total water concentration can be written

$$C_{w,0} = C_0 + \frac{1}{2}S_0 = C_0(1 + \frac{1}{2}k_0) \quad (11)$$

again with subscript “0” for disappearing stress.

The ratio of total water concentrations under stress and in the absence of stresses is

$$\frac{C_w}{C_{w,0}} = \frac{1 + \frac{1}{2}k}{1 + \frac{1}{2}k_0} \quad (12)$$

Since the left-hand side is known from experimental data, the stress-enhanced equilibrium constant can be computed as

$$k = (2 + k_0) \frac{C_w}{C_{w,0}} - 2 \quad (13)$$

Experimental results on equilibrium ratios from literature were expressed in [11] for the temperature range of  $90^\circ\text{C} \leq \theta \leq 350^\circ\text{C}$  by the empirical relation

$$k_0 = A \exp\left(-\frac{Q}{RT}\right) \quad (14)$$

( $A=32.3$  and  $Q=10.75$  kJ/mol,  $T=\theta+273^\circ\text{K}$ ). For room temperature, we obtain by extrapolation to  $23^\circ\text{C}$  ( $T=296^\circ\text{K}$ )

$$k_0 = 0.41 \quad (15)$$

With  $C_w/C_{w,0}$ , eq.(13) yields

$$k \cong 222 \Rightarrow \frac{k}{k_0} \cong 540 \quad (16)$$

an enormous increase of the equilibrium ratio by the stress field near the crack tip. The result clearly illustrates the strong effect of tensile stresses. The equilibrium of the reaction (1) is strongly shifted to the right side.

Finally, the hydroxyl concentrations are

$$S(0) = \frac{17}{18} C_w(0) / \left(\frac{1}{2} + \frac{1}{k}\right) = 16.5 [14.4, 18.4] \text{ (wt\%)} \quad (17)$$

and 
$$S_0 = S(0) = \frac{17}{18} C_{w,0} / \left(\frac{1}{2} + \frac{1}{k_0}\right) = 0.0368 \text{ (wt\%)} \quad (18)$$

The factor 17/18 is the ratio of the mole masses of hydroxyl and molecular water. In [12] we derived from the spherical pore model a maximum possible hydroxyl concentration of

$$S_{\max} = 15.7 \text{ [13.3, 19.2] (wt\%)} \quad (19)$$

The 90%-confidence intervals of  $S(0)$  and  $S_{\max}$  from eq.(19) totally overlap, confirming the expectation that hydroxyl concentration at the crack tip is the maximal possible one.

### 3 Sign of the activation volume

The effect of externally applied stresses was derived in [8] for the case of *uni-axial tension*. In this case the hydrostatic stress is only

$$\sigma_h = \frac{1}{3}(\sigma_x + \sigma_y + \sigma_z) = \frac{1}{3}\sigma_y \quad (20)$$

when  $\sigma_y$  is the axial stress.

The near-tip stress state on the prospective plane of a crack is multiaxial. The stresses in the distance  $r$  from the crack tip, caused by the stress intensity factor  $K$ , are

$$\sigma_x = \sigma_y, \quad \sigma_z = 2\nu\sigma_y \quad (21)$$

with 
$$\sigma_y = \frac{K_{ip}}{\sqrt{2\pi r}} \quad (22)$$

Here,  $\sigma_y$  is the stress normal on the crack plane,  $\sigma_x$  the stress in crack propagation direction and  $\sigma_z$  the stress component parallel to the crack front and  $\nu$  is Poisson's ratio,  $\nu=0.17$ .

Consequently, it holds along the later crack surface after crack extension:

$$\frac{\sigma_h}{\sigma_y} = \frac{2}{3}(1 + \nu) \underset{\nu=0.17}{=} 0.78 \quad (23)$$

This value is much closer to the purely hydrostatic stress state described by  $\sigma_h/\sigma_y=1$  and is therefore much more appropriated for crack problems.

In the hydrostatic case, the equilibrium constant for the reaction under pressure  $p$  is

$$\frac{\partial \ln k}{\partial p} = -\frac{\Delta \bar{V}}{RT} \quad (24)$$

with the changes of the total reaction volume  $\Delta \bar{V}$ .

In the case of mechanical stresses, the pressure has to be replaced by the hydrostatic stress  $\sigma_h = -p$

$$\frac{\partial \ln k}{\partial \sigma_h} = \frac{\Delta \bar{V}}{RT} \quad (25)$$

The equivalent representation of eq.(25) is

$$\frac{k}{k_0} = \exp \left[ \frac{\sigma_h \Delta \bar{V}}{RT} \right] \quad (26)$$

where  $k_0$  is the equilibrium constant in the absence of stresses, eq.(14). From (15) and (16) it becomes evident that the strong increase of the equilibrium constants must be caused by a positive reaction volume, i.e.  $\Delta \bar{V} > 0$ . This is in clear contrast to the conclusions by Nogami and Tomozawa [4] (for the discussion of this discrepancy see [13]).

#### 4. Etching

In a further step, the authors of [5] tried etching off the surface layer of the sample prepared by slow crack growth in water. For this purpose, the glass was etched in a 17% HF-65% H<sub>2</sub>SO<sub>4</sub> solution for 20 s at room temperature. In Fig. 2a, the data from [5] are plotted. The circles are measured H-concentrations without etching (see Fig. 1), the triangles represent the profile after etching (unfortunately, the data indicated by triangles also include results for crack surfaces that were obtained in fast tests in a paraffin oil environment).

The shift between etched and non-etched results indicated by the arrows is 3nm. This means that only a very small layer was removed by the etching step, less than probably expected in [5]. This effect is not astonishing, at least not in the light of strong compressive swelling stresses at the crack surface caused by swelling.

The high compressive swelling stresses must of course hinder the etching procedure. This effect may be discussed on results obtained during the studies in [11]. In the hot-water soaking tests on silica disks, the water-affected surface was removed in steps by etching in hydrofluoric acid/sulfuric acid solutions at room temperature in order to measure the curvature change. Since in these tests the change of the bending moment was determined, the surface swelling stresses are available.

In Fig. 2b, the etching rates are plotted as a function of the swelling stress for disks that were soaked for 2 h at about 200°C under saturation water vapour pressure of 1550 kPa. The open circles show results at 216°C, the solid circles stand for a test at 196°C. From this plot we found that the etching rate decreases with increasing compressive swelling stresses. A fit over all data according to

$$\frac{d\delta}{dt} = a_0 \exp[a_1 \sigma_{sw}] \quad (27)$$

resulted in the parameters

$$a_0=0.1179 \mu\text{m}/\text{min} [0.1154, 0.1203], a_1=0.0032 \text{ MPa}^{-1} [0.0024, 0.0041]$$

with the 90% Confidence Intervals in brackets.

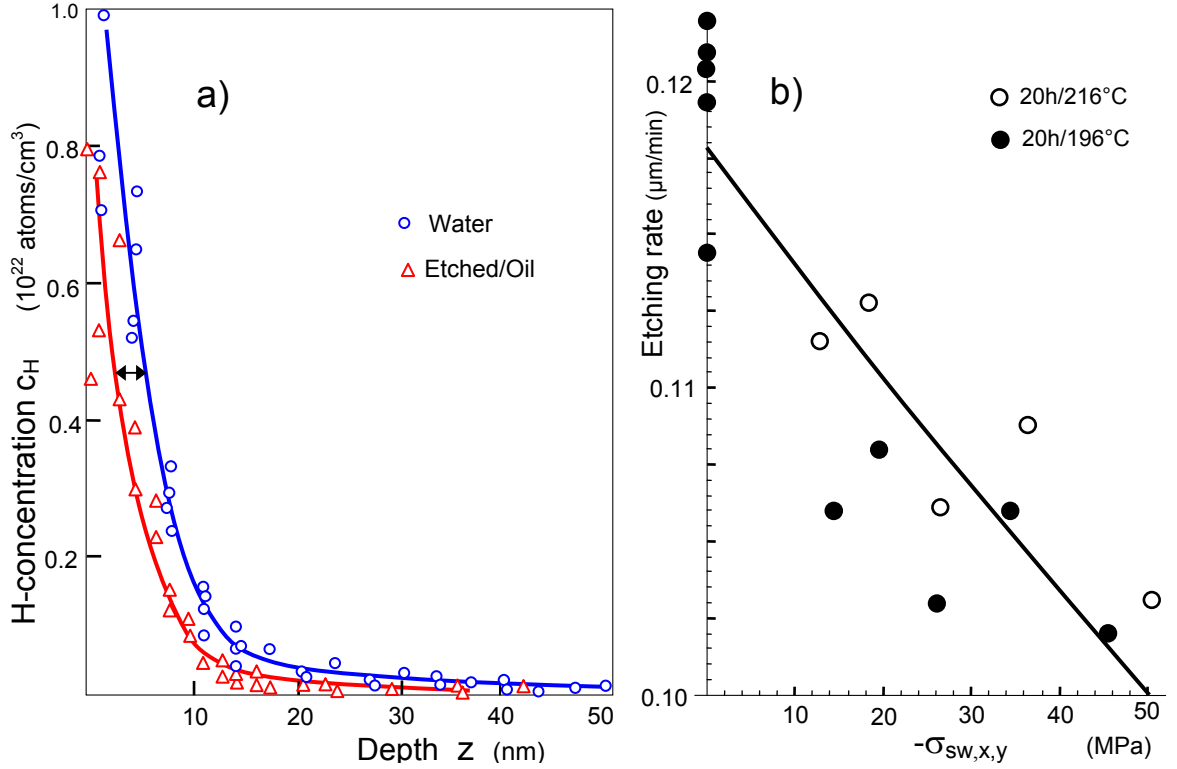


**Fig. 2** a) H-profile after etching (triangles) compared with data before etching (circles), b) etching rate as a function of the average stress in the etching intervals for hot-water soaked silica disks at about 200°C for 20 h.

Since the hydrostatic swelling stress at the surface is 2/3rd of the equi-biaxial stress, a representation via an Arrhenius relation gives the stress dependence of the etching rate by

$$\frac{d\delta}{dt} = a_0 \exp\left(\frac{\sigma_{sw,h} V}{RT}\right) \quad (28)$$

with an activation volume  $V$ ,

$$V=11.7 \text{ cm}^3/\text{mol} [8.8, 15]$$

again with 90% Confidence Interval in brackets.

The hydrostatic swelling stress at a free surface is given by

$$\sigma_{sw,h} = -\frac{2}{9} \frac{E \varepsilon_v}{1-\nu} = -18.7 \text{ GPa} \times S \quad (29)$$

Introducing  $S=0.166$  in eq.(29) yields a hydrostatic swelling stress of  $\sigma_{sw,h} \approx -3.1$  GPa. In this case, eq.(28) would give a practically disappearing etching rate. Even having in mind the rather large data scatter in Fig. 2b and the extremely extended range of application ( $50 \text{ MPa} \Rightarrow 3 \text{ GPa}$ ), we must conclude a strong reduction in etching rates.

### APPENDIX: K evaluation for the DCDC-test

The DCDC-experiments in [5] were claimed to be carried out in a stress intensity factor range of  $0.13 < K < 0.18 \text{ MPa}\sqrt{\text{m}}$ . Figure A1 gives the result from [5]. The test specimen was a rectangular of  $2L=60 \text{ mm}$  length,  $2H=9.4 \text{ mm}$  width with a hole of diameter  $2R=4.4 \text{ mm}$ . The dimensions are illustrated as the insert in Fig. A1. The pressure applied at the ends was  $p=57 \text{ MPa}$ .

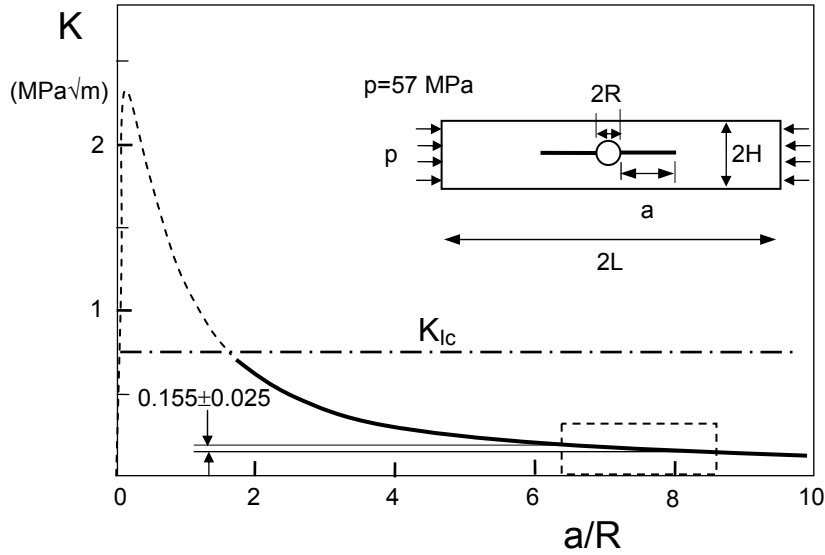


**Fig. A1** Stress intensity factor solution of  $K=0.13\text{-}0.15 \text{ MPa}\sqrt{\text{m}}$  during crack extension in the dotted region for the DCDC-test as claimed by Tomozawa et al. [5]. Insert: DCDC specimen with  $2R=4.4\text{mm}$ ,  $2L=60\text{mm}$ ,  $2H=9.4\text{mm}$ , and end pressure  $p=57 \text{ MPa}$ .

Since the  $K$ -values are very small and incredible, we computed the  $K$ -values once more with published solutions for the DCDC-specimen. For the computation of the stress intensity factor at for instance  $a/R=8.5$  (right end of the dashed box in Fig. A1) we can use many solutions from literature. Here we may apply the solutions by He et al. [14]:

$$K = \frac{|p| \sqrt{\pi R}}{\frac{H}{R} + \left[ 0.235 \frac{H}{R} - 0.259 \right] \frac{a}{R}} \quad (\text{A1})$$

and by Fett et al. [15]

$$K = \frac{|p| \sqrt{\pi R}}{-0.37 + 1.116 \frac{H}{R} + \left[ 0.216 \frac{H}{R} - 0.1575 \right] \frac{a}{R}} \quad (\text{A2})$$

The results are from eq.(A1):

$$K=1.12 \text{ MPa}\sqrt{\text{m}}$$

and from eq.(A2):

$$K=1.03 \text{ MPa}\sqrt{\text{m}}$$

both clearly above fracture toughness  $K_{Ic}$ . Because of these values we have doubt on the measurements. The reason for the discrepancies can only clarify the authors of [5]. The fact that the Sammis and Ashelby [16] stress intensity factor solution is wrong has been stated early by Michalske et al. [17] however after the appearance of [5]. Michalske et al. compared their results from FE-computations on a specimen with  $H/R=3.75$  with results from [16]. Strong deviations were found as can be seen from Fig. A2.

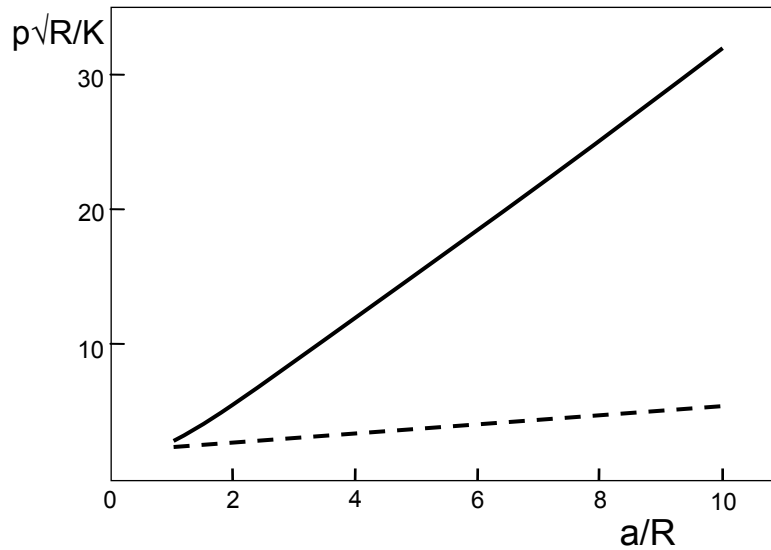


**Fig. A2** Comparison of the solution by Sammis and Ashby [16] (dashed line) with a FE-solution for  $H/R=3.75$  by Michalske et al. [17] (solid curve). Enormous deviations by factors up to six are visible.

The crack-growth data by Wiederhorn and Bolz [18], measured with the DCB-method, would give by extrapolation to  $0.18 \text{ MPa}\sqrt{\text{m}}$ :

$$v < 10^{-18} \text{ m/s}$$

Tomozawa et al. [5] only mention, “the crack velocity for silica glass in water under this stress intensity is not known but is expected to be slow”.

## References

---

- 1 H. Le Chatelier, *C.R. Acad. Sci. Paris* **99**(1884), 786
- 2 R.H. Doremus, "Diffusion of water in silica glass," *J. Mater. Res.*, **10** 2379-2389 (1995).
- 3 S. M. Wiederhorn, G. Rizzi, S. Wagner, M. J. Hoffmann, and T. Fett, Stress-Enhanced Swelling of Silica: Effect on Strength, *J. Am. Ceram. Soc.* **99**(2016), 2956-63.
- 4 M. Nogami, M. Tomozawa, Diffusion of water in high silica glasses at low temperature, *Phys. and Chem. of Glasses* **25**(1984), 82-85.
- 5 M. Tomozawa, W.-T. Han and W.A. Lanford, "Water Entry into Silica Glass during Slow Crack Growth," *J. Am. Ceram. Soc.* **74** [10] (1991) 2573-2576
- 6 C. Janssen, in *Proceedings of Tenth International Congress on Glass, Kyoto, Japan 1974*. (Ceramic Society of Japan, Tokyo, Japan 1974) p. 10.23
- 7 Michalske, T.A., Smith W.L. and Chen, E.P. "Stress Intensity Calibration for the Double Cleavage Drilled Compression Specimen," *Eng. Frac. Mech.* **45**(1993), 637-42.
- 8 S. M. Wiederhorn, T. Fett, G. Rizzi, M. J. Hoffmann, J.-P. Guin, The Effect of Water Penetration on Crack Growth in Silica Glass, *Engng. Fract. Mech.* **100**(2013), 3-16
- 9 Zouine, A., Dersch, O., Walter, G., Rauch, F., Diffusivity and solubility of water in silica glass in the temperature range 23-200°C, *Phys. Chem. Glasses*, **48** (2007), 85-91.
- 10 N.P. Bansal and R.H. Doremus, *Handbook of Glass Properties*, Academic Press, Inc. Orlando, FL (1986).
- 11 S. M. Wiederhorn, F. Yi, D. LaVan, T. Fett, M.J. Hoffmann, Volume Expansion caused by Water Penetration into Silica Glass, *J. Am. Ceram. Soc.* **98** (2015), 78-87.
- 12 S. M. Wiederhorn, G. Schell, M. J. Hoffmann, and T. Fett, Effect of Damage in Surface Layers of Silica on Strength, *J. Am. Ceram. Soc.* (under Review).
- 13 S. M. Wiederhorn, G. Rizzi, S. Wagner, G. Schell, M. J. Hoffmann, T. Fett, Diffusion of water in silica: Influence of moderate stresses, *J. Am. Ceram. Soc* **101**(2018), 1180-90.
- 14 He, M.Y., Turner, M.R., Evans, A.G., Analysis of the double cleavage drilled compression specimen for interface fracture energy measurements over a range of mode mixities, *Acta metall. mater.* **43**(1995), 3453-3458.
- 15 T. Fett, G. Rizzi, D. Munz, T-stress solution for DCDC specimens, *Engng. Fract. Mech.* **72**(2005), 145-149.
- 16 C. G. Sammis and M. F. Ashby, The failure of brittle porous solids under compressive stress states. *Acta Metall.* **34**, 511-526 (1986).
- 17 Michalske, T.A., Smith, W.L., Bunker, B.C., Fatigue mechanisms in high-strength silica-glass fibers, *J. Am. Ceram. Soc.*, **74**(1991), 1993-96.
- 18 Wiederhorn, S.M. and Bolz, L.H., Stress Corrosion and Static Fatigue of Glass, *J. Am. Ceram. Soc.* **53**[10] (1970) 543-549.



KIT Scientific Working Papers  
ISSN 2194-1629

[www.kit.edu](http://www.kit.edu)